USING SURFACTANT-BASED COLLOIDAL SYSTEMS TO PROMOTE PHOTOINDUCED SYNTHESIS OF SILVER NANOPARTICLES

A Thesis by

Shan Shi

Bachelor of Science, Rouen University, 2012

Submitted to the Department of Chemistry
and the faculty of the Graduate School of
Wichita State University
in partial fulfillment of
the requirements for the degree of
Master of Science

July 2018

USING SURFACTANT-BASED COLLOIDAL SYSTEMS TO PROMOTE PHOTOINDUCED SYNTHESIS OF SILVER NANOPARTICLES

The following faculty members have examined the final copy of this thesis for form and content and recommend that it be accepted in partial fulfillment of the requirement for the degree of Master of Science with a major in Chemistry.

_____

Douglas S. English, Committee Chair

_____

David M. Eichhorn, Committee Member

_____

Katie Mitchell-Koch, Committee Member

_____

Kandategе Wimalasena, Committee Member

_____

Leland Russell, Committee Member

DEDICATION

To my parents and dear friends.

ACKNOWLEDGEMENTS

I would like to thank my advisor, Dr. Douglas S. English, who made it possible for me to complete this thesis. His support, knowledge, and patience have guided me from the very beginning to the end. I would also like to thank Dr. David M. Eichhorn, Dr. Katie Mitchell-Koch, Dr. Kandategе Wimalasena and Dr. Leland Russell for their kind help and for serving on my thesis committee. In addition, I would thank my lab mate Thanh Dinh for his help on my research. Finally, I would like to thank my parents, Jianyue Shi and Cong Zhang, and my husband, Shuang Xia for their endless support and encouragement.

ABSTRACT

This thesis focuses on the photo-initiated synthesis of silver nanoparticles in water with low concentration of stabilizing agents to investigate the role that surfactants, specifically their charge, plays in the synthesis. The employed stabilizing agents include sodium dodecyl sulfonate (SDS), sodium-dodecyl-benzenesulfonate (SDBS), and cetyltrimethylammonium tosylate (CTAT) surfactants along with SDBS-rich and CTAT-rich surfactant vesicles. The formation of silver nanoparticles is monitored by the color change of the reaction mixture from clear to yellow that arises from the onset of a strong, visible absorption band that is due to the surface plasmon resonance (SPR) that is characteristic of AgNPs. By comparing the product generated from different stabilizers, we found that above the critical micelle concentration (CMC), both negatively charged surfactants, SDS and SDBS, work well for promoting the formation of AgNPs whereas the positive charged surfactant, CTAT, is not suitable for the synthesis. With SDS and SDBS, the anionic interface recruits silver cations in a counter-ion cloud around the micelle and also provides a passivating layer to limit the growth of the nanoparticle. The use of vesicle-forming, mixed-surfactant preparations was also investigated using both SDBS-rich and CTAT-rich mixtures. It was found that while SDBS-rich vesicles are optimal for preparing AgNPs with a distinct SPR band and good yield, CTAT-rich vesicles result in AgNPs with a broad SPR band characteristic of a polydisperse preparation. The SDBS-rich vesicles are therefore deemed the best formulation for yielding AgNPs since it has high yield with minimal added surfactant due to the micromolar critical aggregation concentration (CAC), and the ability to recruit more silver cations at the bilayer interface. This result is valuable since the use of less surfactant could be advantageous from a cost perspective and if the goal is to produce samples with minimal surfactant in the product.

TABLE OF CONTENTS

TABLE OF CONTENTS (continued)

Chapter Page

LIST OF FIGURES

LIST OF FIGURES (continued)

Figure Page

LIST OF TABLES

Table Page

LIST OF ABBREVIATIONS

Abbreviation	**Systematic name**
AgNPs	Silver Nanoparticles
AuNPs	Gold Nanoparticles
CAC	Critical Aggregation Concentrations
CMC	Critical Micelle Concentration
C_{pp}	Critical Packing Parameter
CTAT	Cetyltrimethylammonium tosylate
I-2959	2-hydroxy-4'-(2-hydroxy-ethoxy)-2-methyl propiophenone
PC	Phosphatidylcholines
PDDA	Polyn(diallyldimethyldi- methylammoniumchloride)
PVP	Polyvinylpyrrolidone
SDBS	Sodium dodecylbenzenesulfonate
SDS	Sodium dodecyl sulfate
SEC	Size-exclusion chromatography
SPR	Surface Plasmon Resonance
TOAB	Tetrabutylammonium bromide
Triton 100	Octyl phenol ethoxylate

CHAPTER 1

SILVER NANOPARTICLES (AgNPs)

1.1 Introduction of Nanoparticle Chemistry

1.1.1 Background of Metal Nanoparticles

'Nano' is derived from a Greek word for 'dwarf' and used to describe a material which is extremely tiny. Therefore, it is not visible to the naked eye. Nanoparticle typically refers to particles with sizes between 1 to 100 nm. Metal nanoparticles are metal particles in the nanoscale. The most common metallic nanoparticles are gold, silver, copper, and iron oxide nanoparticles which have been studied and utilized for centuries. The usage of metal nanoparticles can be dated from late Roman times. The most famous examples are the Lycurgus Cup[1] (Figure1A) and Stained glass windows [3] (Figure1B). The Lycurgus Cup is made of glass. It is unique since it appears green when illuminated from the front, but red when lit from behind. This surprising color variation is due to the addition of gold and silver nanoparticles during the preparation of the glass. Stained-glass windows are colorful and widely used in ornate cathedrals of Europe. The red color of stained glass is due to gold nanoparticles immersed in glass, while the yellow color is because of added silver nanoparticles. These startling artistic effects were not attributed to metallic nanoparticles until the mid-nineteenth century although they had been used for hundreds of years. In 1857, these peculiar optical effect from gold nanoparticles was proved in Faraday's paper,[4] then it was also confirmed in other nanoparticles like silver. In fact, the plasmon absorption was responsible for variable colors of metal nanoparticles in glass. This unique propriety will be introduced in section 1.1.4 and is known as the surface plasmon resonance effect or SPR.[5-8]

Silver is a noble metal which has been used for thousands of years, particularly for its

antibacterial properties. As early as ancient Rome, people started to preserve drinking water and food in containers made of silver, and this method was still used during World War II.[9] Another example is using silver nitrate eye drops to prevent ophthalmic infections for newborns in the 1880s.[10] In the past few decades, with the advent of nanoscience, silver nanoparticle or colloidal silver have gained increasing attention. Colloidal silver refers to silver nanoparticles that are dispersed and stable in solution. Researchers find that colloidal silver has higher antibacterial activity due to the small size and high surface area which reduces the silver concentration required for these applications. However, the toxicity of AgNPs still limits its usage. In addition, because of the smaller size, colloidal silver, as well as other metal nanoparticles, possess several specific physical properties, resulting in the wide range of applications in various fields such as textiles,[11] food storage,[12] painting,[13] drug delivery,[14] and therapy.[14]

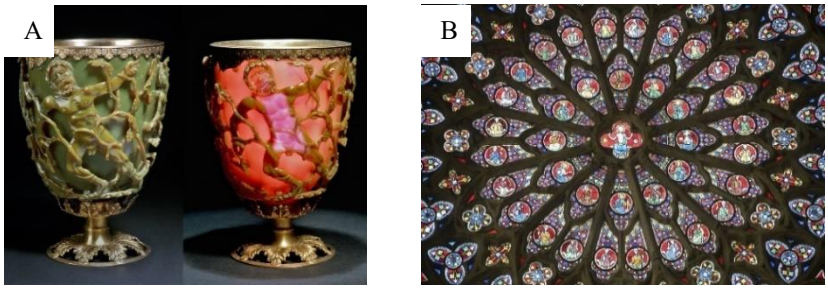

Figure 1. A) Roman Lycurgus cup.[1] B) Stained-Glass Window[3]

1.1.2 Unique Propriety of Silver Nanoparticles

Compared with bulk metal, silver, as well as other metallic nanoparticles have unique proprieties which lead to a diversity of applications. First, a silver nanoparticle has a high surface to volume ratio which increases its reactivity. Small particles have larger surfaces that contact and react with surrounding materials thus increasing their reactivity. Second, nanosilver or other silver-involved compounds possess exclusive antibacterial properties which can be used to control

bacterial growth. The antibacterial effect is because of the sustained release of silver ions from the nanoparticles.[14] Silver ions cripple enzymes which are employed by bacteria or fungui to metabolize oxygen, thereby killing the bacteria in several minutes without affecting surrounding tissues. Third, silver nanoparticles have remarkable optical properties which lead to various colors of colloidal silver, and the color of the solution highly depends on particle size and shape.[7-8] This property stems from surface plasmon resonance effect. Surface plasmon resonance is a special physical phenomenon of metal nanoparticles and will be discussed separately in section 1.1.4. Fourth, as the particle size decreases, its melting point decreases, which suggests utility for electrical applications. For instance, AgNPs smaller than 10 nm are favored for making electronic contacts.[15] Fifth, AgNPs with extremely small size (<1 nm) have unusually high superconductivity transition temperature and can be used for making high-temperature superconductivity materials.[15]

1.1.3 Applications of Silver Nanoparticles

Owing to these remarkable properties, especially for antibacterial and optical purposes, there are numerous AgNP applications emerging in various fields. The distinctive antibacterial activity of AgNPs are widely applied in consumer goods.[16] For example, adding AgNPs in clothing (T-shirts and socks), personal care product (toothpaste), household product and appliance surfaces (trash bag, hair straighter and refrigerator surface) helps to kill bacteria and extend products' use time. Also, many biomedical applications are developed from its antibacterial activity.[17] For instance, adding AgNPs in dental filling material enhances its bactericidal effects. Contact lenses containing nanosilver reduce bacterial colonization and are beneficial for long-term use.[18] Due to the unique optical properties, AgNPs are available as a biosensor or bioimaging agent.[19] When silver nanoparticles bind with biomolecules, the absorption and scattering effect becomes stronger and a shift in the plasmon band wavelength is observed. This shift can be used to identify properties

of biomolecules. For example, bovine serum albumin is detected by the biosensor consisting of silica-coated nanosilver.[20] AgNPs are also a tool for in vivo therapy.[19] They absorb light when binding with biological targets such as cancer cells and convert light to thermal energy hence destroying the target by thermal ablation.[19]

1.1.4 Surface Plasmon Resonance Effect

Silver nanoparticle or other metallic nanoparticle is also called a plasmonic nanoparticle since its unique optical property originates from the Surface Plasmon Resonance Effect (SPR). What is SPR? To answer this question, we should know what plasma and plasmon are first. Plasma is the 4th state of matter apart from solid, liquid and vapor.[21] It consists of charged (both positive and negative) particles. The number of positive and negative charge particles are identical so that the whole system is neutral. Metals resemble a plasma in that, while the positively charged nucleus is fixed in the crystal lattice, electrons can occupy the conduction band, delocalize and act collectively. The plasmon is the collective oscillation of electrons in the conduction band when excited by incoming light. Surface plasmon is a plasmon which is confined to the surface. While the incident light excites conductive electrons, an electromagnetic wave is generated at the interface of metal and dielectric, and it propagates parallel to the metal surface. If the size of metal nanoparticles is smaller than the wavelength of incident light, the frequency of oscillation will coincide with the visible light region. The incoming light resonates with surface plasmon oscillation when the frequency of incoming light and frequency of collective oscillation matches each other. This physical phenomenon is defined as the surface plasmon resonance effect and is shown in Figure 2. This effect leads to an unusually strong response (scattering and absorption of light), and this response can be detected spectroscopically. The electron oscillation of silver nanoparticles is strong and easily detected by UV-vis spectroscopy around 400 nm. Therefore,

colloidal silver exhibits the yellow color which is the complementary color to blue. As particle size dispersity increases, the SPR absorption band becomes broad and featureless, lacking the sharp band characteristic of nanoparticles, and the solution color changes to brown.

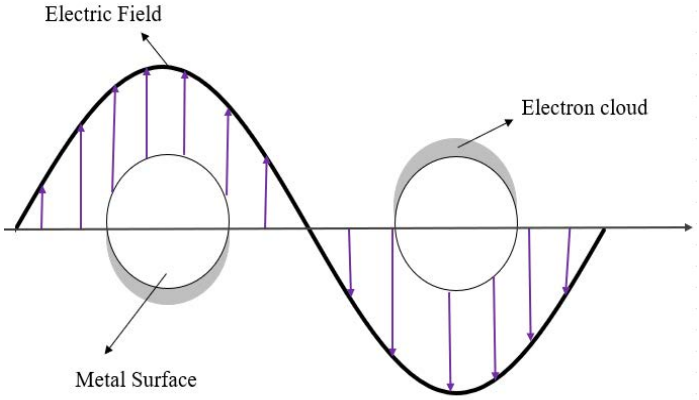

Figure 2. Theory of Surface plasmon resonance effect

The position and width of the surface plasmon absorption band are affected by the size, shape, and aggregation state as well as surrounding environment of metal nanoparticles.[6-7, 22] In general, the intensity of SPR peak increases with the increasing particle concentration and shifts with size. The SPR band shifts to longer wavelength (red shift) as particle size increases. A narrow and symmetric peak indicates nanoscale particles with low size dispersion.[7] When small particles aggregate, ripen to larger sizes or become polydisperse, this results in a broader peak. Compared with other metal nanoparticles like gold, silver nanoparticles have a sharper and more intense SPR band since there is a small overlap between the surface plasmon and interband transition from 320 nm, which leads to a different dielectric environment.[6] In addition, nanoparticle shape alters the SPR band by affecting the surface polarization. The surrounding environment or solvent also affects the spectral band. For instance, the spectral band shifts when the silver nanoparticles are redispersed from THF to toluene.[23] In addition, AgNPs, which are produced and kept in various pH solutions, have different (redshift or blueshift) plasmonic bands.[22] This is because of the

variable size of generated particles. The particle size increases as pH rises, resulting in a redshift of the plasmon peak.

1.2 Methods of Silver Nanoparticle Synthesis

Synthetic methods for preparing silver nanoparticles have been widely investigated from the beginning of this century. In general, the approaches can be sorted into two classes: Top-down or Bottom-up.[24] In nanoparticle synthesis, top-down process is defined as starting with bulk material and reducing it to nanoparticles. Bottom-up starts from molecules, and then generates nanoparticles. The top-down process usually relates to a physical approach that involves input of energy such as annealing and vapor condensation.[24] The physical approach generally has short processing time but high energy consumption. It generates AgNPs with narrow size distribution without using toxic chemicals. Chemical and biological methods belong to the bottom-up process. All bottom-up processes involve redox reactions. Due to the relatively large electropositive reduction potential of silver (Ag^+/Ag^0 in H_2O, $E^0 = +0.799$ V),[25] silver salts are eligible to react with reducing agents, therefore, generating Ag(s). The reducing agent could be chemicals such as sodium citrate ($E^0 = -0.180$ V), sodium borohydride ($E^0 = -0.481$ V), or a plant such as leaf extract of azadirachta indica.[26] Ag^+ is reduced to Ag^0, and as Ag^0 accumulates into nanoscale, silver nanoparticles are formed. Aggregation of nanoparticles is a significant issue during synthesis.[27] As silver ions are reduced to silver atoms, solid crystalline silver is formed and can easily gain particle size beyond the nanoscale. In order to avoid aggregation or gain the nanoparticle with designed size, a stabilizer should be added during synthesis. Surface coatings are typically utilized to stabilize nanoparticles. Nanoparticle aggregation is avoided by enhancing the electrostatic, steric, or electrosteric repulsive force between nanoparticles.[27] These approaches are illustrated in Figure 3. Surfactants stabilize AgNPs through electrostatic repulsion. Polymers enhance the steric

effect between coated nanoparticles. Polyelectrolytes reinforce both electrostatic repulsion and steric effect and thereby stabilizing AgNPs through electrosteric repulsive force. For example, Sodium dodecyl sulfate (SDS), structure is shown in Figure 3A, is a negatively charged surfactant which binds with nanoparticles to reinforce surface charge and electrostatic repulsion, thus increasing the stability of nanoparticles in solution. Polyvinylpyrrolidone (PVP), whose structure is shown in Figure 3B, is an environmentally friendly polymer, which has relatively larger molecular weight, creating steric repulsion between coated nanoparticles to prevent aggregation. Poly (diallyldimethyldi-methylammonium chloride) (PDDA), whose structure is shown in Figure 3C, is a positively charged ionic polymer that avoids aggregation via electrosteric repulsion.[27]

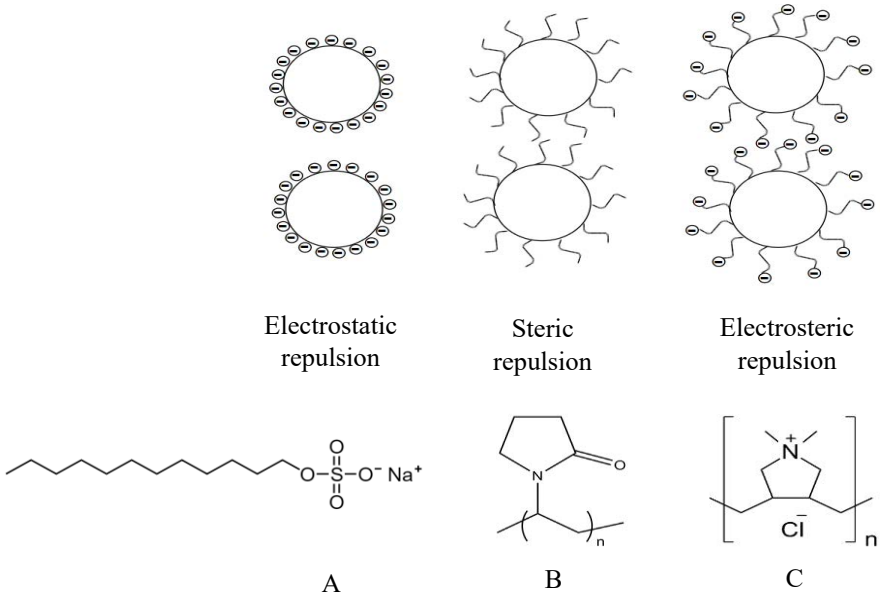

Figure 3. Three types of interparticle repulsion provided by the surface coating molecules. Examples A) Chemical structure of SDS. B) Chemical structure of PVP. C) Chemical structure of PDDA.

1.2.1 Common methods via chemical reduction

Chemical reduction is the most common method for preparing silver nanoparticles. There

are three components included for the syntheses in solution: Ag^+ salts which provide the silver source, reducing agent and stabilizing or capping agent. Various chemicals can be employed as a reducing agent such as citrate ion, $NaBH_4$, hydroquinone and gallic acid.[24] As silver ions are reduced to Ag^0, they accumulate to form AgNPs and may grow into a larger size. Capping agents control the size growth and keep particles in optimal size.

The Turkevich[28] method and Brust[29] methods are well-known for the metal nanoparticle synthesis. The Turkevich method was reported in 1951 for synthesizing colloidal gold at elevated temperatures, using trisodium citrate. The particle size is around 20 nm. The mechanism is shown in Figure 4. Frens improved this method in 1973 by varying the citrate to gold ratio and obtained AuNPs from 15 to 50 nm.[30-31] This method has been extended to make nanosilver and other nanometals. In this method, citrate ion apparently acts as both reducing agent and stabilizer. Interestingly, using gold, researchers found that in the initial step of the process, there are two reactions occurring simultaneously: as Au^{3+} is reduced to Au^0, citrate is oxidized to dicarboxy acetone.[27] This suggests that the actual stabilizer in the reaction is dicarboxy acetone rather than the citrate ion itself. However, due to the apparently dual function of citrate anions, it's hard to fully understand how citrate affects reduction and stabilization separately. Natan's group introduced a method using $NaBH_4$ to reduce Au^{3+} and citrate only as a stabilizer.[32] Due to the stronger reducing strength of $NaBH_4$, this reaction occurs at room temperature and the size of particles shrinks to 6 nm.

The Brust-Schiffrin method was published in 1994.[29] It synthesized small size (less than 5 nm) thiolate-stabilized AuNPs at room temperature. The average size of obtained AuNPs is controlled by adjusting the Au^{3+} to thiol ratio. There are 3 steps included in the reaction. First, transfer Au^{3+} to organic solvent like toluene with the help of a phase transfer agent

tetrabutylammonium bromide (TBAB), second, add thiols for reducing Au^{3+} to Au^{+}; and third, Au^{+} is reduced to Au^{0} by adding $NaBH_4$ in the presence of a thiol group which leads to the formation of AuNPs. The only difference for the AgNPs synthesis is that the thiol group just acts as a capping agent which forms a monolayer on the silver surface.

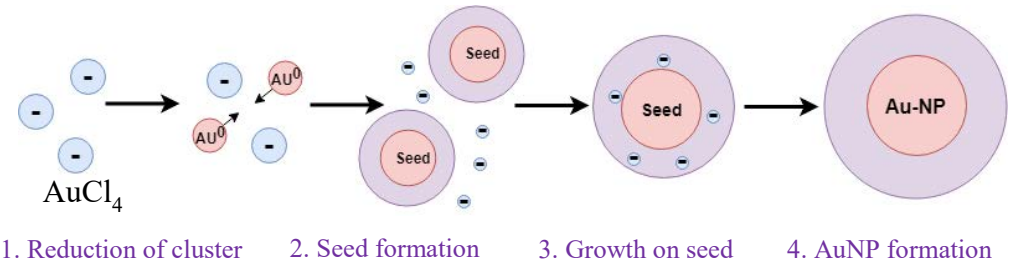

Figure 4. General mechanism of Turkevich method.

1.2.2 Photochemical Method

Light-assisted chemical synthesis offers a simple and green approach which activates the redox reaction by irradiation to generate metal nanoparticles. This is the method applied in this thesis work and employs a photo-initiator (I-2959) that can reduce silver ions to silver atoms (Ag^{0}) by irradiation. In this section, we will introduce how to gain AgNPs starting from I-2959.

I-2959, 2-hydroxy-4'-(2-hydroxy-ethoxy)-2-methyl-propiophenone, whose structure is shown in Figure 5, is a photoinitiator which provides ketyl radicals by the photocleavage reaction.[23] There are three factors that make I-2959 a valuable tool for nanoparticle synthesis. First, I-2959 has strong absorption in the UV region. Therefore, it is easily detected and controlled. Second, it is a widely used photoinitiator and inexpensive. Third, it is soluble in diverse solvents such as water, toluene, acetone, and THF. The ketyl radical is a strong reducing agent which reduces Ag^{+} to Ag^{0}. Due to the presence of a stabilizing agent in the reaction, stable colloidal silver is formed as Ag^{0} accumulates. The reaction scheme is shown in Figure 5. This method has been

intensively studied by Scaiano's group.[23, 33-35] They tried this process in different solvents such as water, toluene and THF, with diverse silver salts and various stabilizers like citrate ions,[35] micelles,[34] and primary amines.[23] This method works in most cases and the size of obtained AgNPs is smaller than 10 nm. In addition, they found most silver salts such as $AgNO_3$, leading to non-fluorescent AgNPs, whereas silver trifluoroacetate produces remarkable fluorescent AgNPs when cyclohexylamine is employed as stabilizing agent.[23] Moreover, to obtain high yield AgNPs, removing oxygen is recommended before illumination. Otherwise, the ketyl radicals will be used to consume the dissolved oxygen in the mixture.[23]

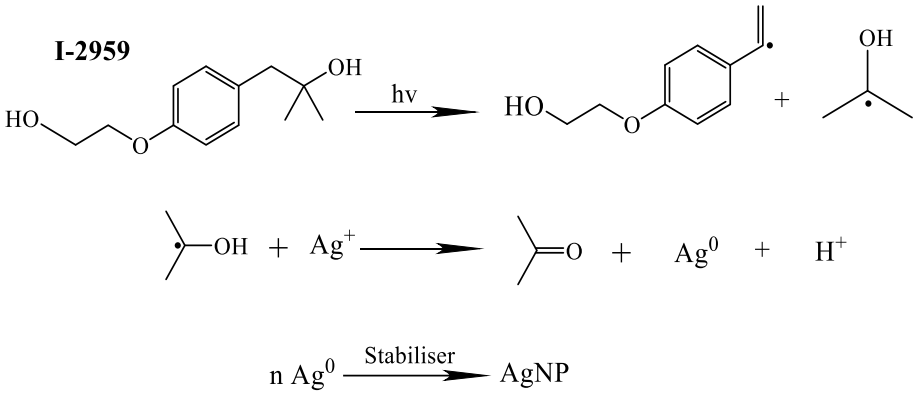

Figure 5. Reaction for the formation of silver nanoparticles from I-2959.

1.3 Thesis goals

In this project, we aim to improve Scaiano's method, synthesizing silver nanoparticles in aqueous solutions with low concentration of stabilizing agents, and to investigate the role that surfactant charge plays in the photo-initiated synthesis of AgNPs.

Although the I-2959 involved irradiation-assisted method used by Scaiano's group is simple and versatile, AgNPs are generated in organic solvents such as toluene. By developing methods to synthesize these particles in water, the methods become less expensive and green.

CHAPTER 2

SURFACTANT - BASE COLLOIDAL SYSTEM

2.1 Introduction of surfactant-base colloidal

Colloids are particles with size between 1 nm and 1 um (10^{-6}-10^{-9} m). Silver nanoparticles that are dispersed in solution is an example of a colloid, so-called colloidal silver. Surfactant is the abbreviation of surface-active agent, which is another class of colloids.[36] Surfactants tend to accumulate or absorb at a surface/interface and alter the surface property and lower the free energy of the surface. In chemistry, interface refers to a boundary between two immiscible phases and surface specifies that one of the phases is gas.[36] The adsorption behavior of surfactants is due to its distinctive chemical structure which is shown in Figure 6, a hydrophilic/polar group and a hydrophobic/nonpolar group coexist in one molecule, exhibiting dual nature, so called amphiphile. "Amphiphile" is a Greek word, Amphi denotes double, and phile means loving. The polar head of a surfactant has higher affinity with polar solvents such as water and alcohol, whereas the nonpolar tail prefers to stay in nonpolar solvents such as alkanes and benzenes. Therefore, surfactants are able to be absorbed on the surface of both polar and nonpolar solvents. At low concentrations, surfactants in water lower their free energy by accumulating at the solution surface where the tail groups are exposed to air and the head group to water molecules. Similarly, in oil the polar head

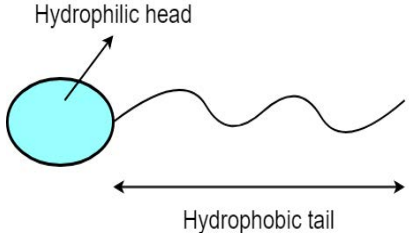

Figure 6. Animation of typical surfactant structure.

is unstable, resulting in a migration towards the surface, thus removing non-favorable interactions and lowering the system's free energy.

Table 1. Example of 4 types of surfactants

	Name	Structure
Cationic	cetyltrimethylammonium tosylate (CTAT)	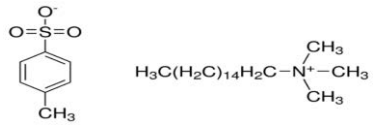
Anionic	sodium-dodecylbenzenesulfonate (SDBS)	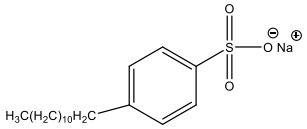
Zwitterionic	phosphatidylcholines (PC)	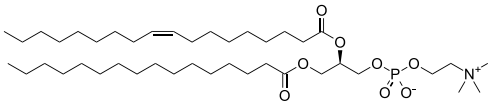
Nonionic	octyl phenol ethoxylate (Triton X-100)	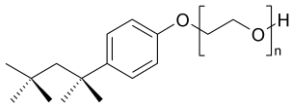

Based on the property of the polar head, surfactants can be classified into four categories: non-ionic, anionic, cationic and zwitterionic, examples are shown in Table 1. Nonionic surfactants are neutral, including ethylene oxide chains or hydroxyl groups in the hydrophilic part such as octyl phenol ethoxylate (Triton X-100), They are generally less reactive than ionic surfactants. Anionic surfactants consist of negatively charged head groups with a positively charged counterion such as sodium-dodecylbenzenesulfonate (SDBS). Cationic surfactants are generally formed by positively charged headgroups with a negative counterion, such as a quaternary ammonium with a halide ion like cetyltrimethylammonium tosylate (CTAT). Zwitterionic surfactants include both negative and positive charge groups such as phosphatidylcholines (PC) that acts as an anion in high pH and a cation in low PH. In addition, surfactants can be sorted into two classes based on

their source: natural surfactants and synthetic surfactants.[36] Phospholipids in mammalian cells are an example of natural surfactants. They are primary amphiphiles in the cell membrane. The formation of cell membrane bilayer is due to the self-aggregation and self-assembly of surfactants. Detailed information will be introduced in section 2.3 “Overview of vesicles”. Synthetic surfactants are produced by multiple chemical reactions from organic compounds such as alkyl benzenes, alcohols, and carbohydrates. Detergent, mainly consisting of surfactants, is the best example of synthetic surfactants.

2.2 Micelles

Surfactants have two specific features. One is that they can be absorbed on surfaces, which we know from section 2.1, another one is that they are able to self-aggregate in solution, thereby decreasing the free energy of the system. Micelles are formed by the self-aggregation of surfactants. At low concentration, surfactants are favorably absorbed on the solution surface. With increasing concentration of surfactants, the absorption on surfaces become stronger, leading to monolayer formation. Any additional surfactants will be retained in the aqueous phase and exist as free molecules. When surfactant concentration in solution becomes equal to or greater than a specific

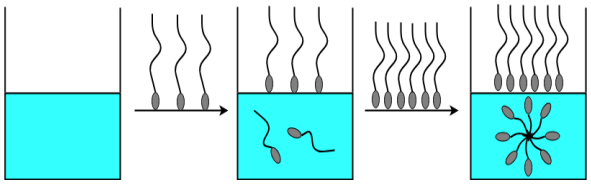

Figure 7. Process of micelle formation

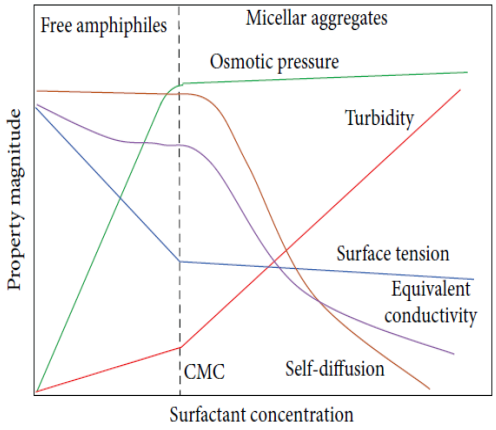

Figure 8. Example of physical property variation at CMC[2]

value, the surfactant molecules will self-aggregate to form micelles. Figure 7 schematically shows how surfactants exist in solution. This specific concentration is called critical micelles concentration (CMC).[2, 36] CMC is a significant parameter of any surfactant. At or above CMC, the physical properties of surfactants in solution change dramatically. Many physical property variations of surfactants are detectable when the CMC is achieved. Figure 8 illustrates a plot of physical properties of the solution versus the surfactant concentration.[2] It clearly demonstrates discontinuous data around CMC. The most common techniques for determining CMC are shown in the same figure.

Micelles have different sizes and shapes because of the molecular geometry of surfactants and solution properties.[36] There are 5 types of aggregates that can be classified by the critical packing parameter (C_{PP}), first described by Israelachvili in 1976.[37]

$$C_{pp} = \frac{V}{a_0 l_c} \tag{2.1}$$

Where V is the volume of the hydrophobic tail, l_c is the chain length of the hydrophobic tail, and a_0 is the surface area of the hydrophilic head on the solution surface. The C_{pp} of most single tail surfactant molecules are less than 1/3 and which predicts the formation of spherical micelles. Cylindrical micelles are formed when C_{pp} is between 1/3 and1/2. For C_{pp} between 1/2 and 1, the curved bilayer leads to the formation of vesicles. A Planar bilayer, a structure similar to a cell membrane, is formed at C_{pp}=1, When C_{pp} is greater than 1, inverse micelles are formed in nonpolar solvents.

2.3 Vesicle

2.3.1 Overview of Vesicles

From the critical packing parameter (C_{pp}) which is discussed in section 2.2, we know that

vesicles are the aggregates which are formed when the C_{pp} is between 1/2 and 1. However, compared with micelles, vesicles have a bilayer (an outer layer and an inner layer), which results in a hydrophobic core and a hydrophilic ring. Vesicles have a spherical bilayer that encloses an interior volume of water within the sphere, and that volume is separated from the surrounding aqueous solution by the bilayer wall. Vesicles composed of phospholipid bilayers are often referred to as liposomes.[38] The unique difference between liposomes and simple vesicles are the chemical composition of the amphiphilic molecules. Liposomes are formed from phospholipid molecules, so-called lipid vesicles.[38] Other vesicles are formed from some other surfactant mixtures. Most phospholipid molecules have non-polar double-tails. Compared with single tail surfactants, they possess larger tail volume, leading to a larger critical packing parameter, therefore, forming vesicles. Liposomes were first reported by Bangham in the 1960s.[39] He revealed that liposomes are the smallest spherical-shape artificial vesicles, produced from natural phospholipids. Since the bilayer of lipid vesicles is similar to a cell membrane, they have been extensively studied and prepared from a variety of lipids and lipid mixtures.

Vesicles can be categorized into four classes.[38] First, vesicles formed from phospholipids, glycolipids, or their mixtures, called lipid vesicles. Second, vesicles formed by the mixture of a nonionic surfactant and an ionic surfactant. Third, vesicles formed by double-chain dialkyldimethylammonium surfactants with halide counterions. Fourth, vesicles formed from mixtures of oppositely charged surfactants in solution are referred to as “catanionic” vesicles. CTAT/SDBS catanionic vesicles are employed in this project and are discussed in the next section.

2.3.2 Spontaneous Formation of CTAT/SDBS Catanionic Vesicles

Catanionic vesicles are formed by mixing cationic and anionic surfactants with an unequal molar ratio in aqueous solution. It was first reported by Kaler in 1989.[38, 40] Since then numbers of

research efforts have focused on this topic, and various formulations of catanionic mixtures are reported such as CTAT-SDBS[41-42] and DDAB-SDS.[38]

In our research, CTAT-SDBS vesicles are employed to stabilize synthesized silver nanoparticles in water. Cetyltrimethylammonium tosylate (CTAT) is a cationic surfactant which consists of quaternary ammonium head group and a tail includes a sixteen-carbon alkyl chain. Sodium dodecylbenzenesulfonate (SDBS) is an anionic surfactant which possesses a sulfonate head group and twelve-carbon alkyl chain in the tail. Chemical structures of these two surfactants are shown in Figure 9. Both CTAT and SDBS are single tailed surfactants, forming micelles with critical packing parameters around 1/3. While mixing them together, the electrostatic attraction between the two oppositely charged head groups will combine them together to form ion pair complexes with a double-tail. This complex has a smaller head group, leading to a larger critical packing parameter. The structure of these complexes is similar to a zwitterionic phospholipid molecule with Cpp around 1 and aggregates into bilayer structure.

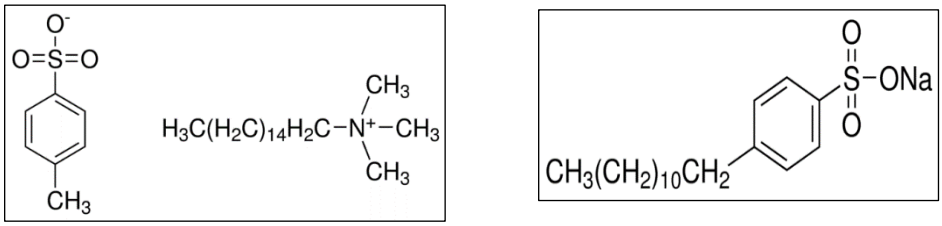

Figure 9. structure of CTAT(left), and structure of SDBS(right)

Since one surfactant (cationic or anionic) should be in excess in the mixture to form a bilayer, the structure of the bilayer possesses paired ion complexes and unpaired surfactants. Therefore, the composition of the inner and outer leaflets of the bilayer are different. The outer leaflet has larger numbers of unpaired surfactants, which leads to greater repulsive interactions

and spontaneous bilayer curvature. This curved bilayer forms stable vesicles, as illustrated in Figure 10.

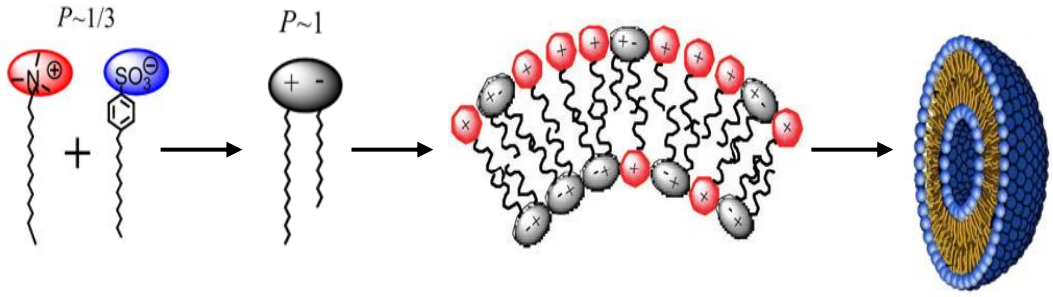

Figure 10. Process of catanionic vesicle formation.

From the description above, we know that a non-equimolar CTAT and SDBS mixture is required for the spontaneous formation of vesicles. However, not all ratios other than 1:1 lead to vesicle formation. A ternary phase diagram for the CTAT and SDBS system, made by Kaler,[40] illustrating the products from different mass ratio mixtures at 25ºC, is shown in Figure 11. The blue region, which is labeled by V^+ and V^- indicates the formation of CTAT-rich, which is positively charged vesicle (V^+) and SDBS-rich, which is negatively charged vesicle (V^-). With the increasing concentration of total surfactants, vesicle, and lamellar phases coexist (grey region). When one surfactant is largely in excess in the mixture, micelles are formed (green region). The 1：1 ratio mixture leads to the precipitation as lamellar solids (along the equal molar line).

Due to the strong attractive interactions between two oppositely charged headgroups, CTAT-SDBS vesicles have a much lower critical aggregation concentration (CAC) than micelles.[42] Critical aggregation concentration is the concentration at which the vesicles start to for, like the CMC for micelles. CMC of CTAT and SDBS surfactants is 0.34 mM[42] and 2.8 mM,[42]

respectively, whereas CAC of CTAT-SDBS vesicle is 2.6μM.[42]

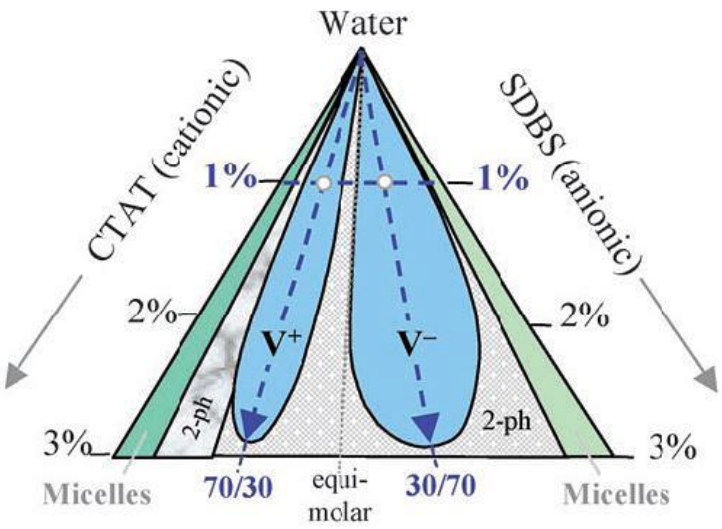

Figure 11. Ternary phase diagram for CTAT-SDBS system in water at room temperature.

Figure 11 was adapted from reference [42]

CHAPTER 3

MATERIALS AND METHODS

3.1 Materials

Silver nitrate was purchased from J&S Scientific Inc. 2-Hydroxy-4′-(2-hydroxyethoxy)-2-methylpropiophenone (I-2959, purity = 98%), sodium dodecyl sulfate (SDS, purity > 99%), hexadecyltrimethylammonium p-toluenesulfonate（CTAT, purity > 99%）and Sephadex G-50 were ordered from Sigma-Aldrich. Sephadex G-200 was purchased from Pharmacia Uppsala Sweden. Sodium dodecylbenzenesulfonate (SDBS, purity > 95%）was ordered from Tokyo Chemical Industry, Deionized water was used. All chemicals were used as received, without further purification.

3.2 Methods

3.2.1 General Procedure of AgNPs Synthesis

$AgNO_3$ 18 mM (before mixing), stabilizer solution (one of SDS, SDBS, CTAT surfactant or SDBS/CTAT vesicle), and photoinitiator I-2959 18 mM (before mixing) were added as the writing order and mixed with 1:1:1 volume ratio in UV quality quartz cuvettes with 1 cm path length. The mixture was purged with nitrogen for 20 minutes to remove oxygen. The solution was exposed to UVA light at 350 nm for another 20 minutes. The color change of the mixture suggested the formation of silver nanoparticles. Figure 12 schematically shows the general procedure. Each experiment was repeated at least 3 times to improve the accuracy.

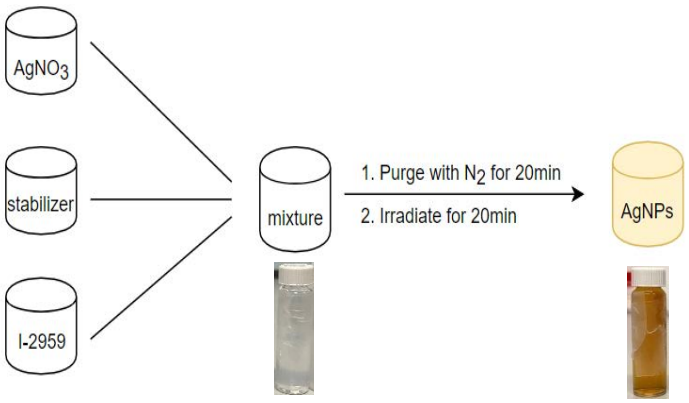

Figure 12. General procedure of AgNPs synthesis

3.2.2 Stock Solution Preparation

$AgNO_3$ (30.6 mg, 18 mM), I-2959 (40.4 mg, 18 mM), SDS (173.0 mg, 60 mM), SDBS (209.0 mg, 60 mM), CTAT (273.4 mg, 60mM) were dissolved in 10.00 mL deionized water separately. Mass ratio CTAT/SDBS vesicles (total surfactant concentration = 60 mM) were prepared by dissolving powder of CTAT and SDBS in 10 mL deionized water with stirring for 15 hours at 25°C. The quantity of SDBS and CTAT are listed in Table 2. Vesicles with total surfactant concentration at 30 mM and 15 mM were obtained by 2-fold and 4-fold dilution of 60 mM vesicles, respectively.

Table 2. Mass required to prepare CTAT/SDBS vesicle.

CTAT/SDBS by mass ratio (Total surfactant concentration= 60mM)		CTAT (mg)	SDBS (mg)
Anionic vesicle	20/80	44.0	175.4
	30/70	67.6	157.4
	40/60	92.4	138.4
Cationic vesicle	60/40	146.3	97.2
	70/30	175.0	75.3
	80/20	206.2	51.4

3.2.3 Size Exclusion Chromatography for AgNPs in CTAT/SDBS 20/80

Size Exclusion Chromatography is a separation technique that separates molecules based on the size. Since the stationary phase contains pores with a defined size range, solutes will go through it at different rates due to their sizes. The largest molecule, which is excluded from pores, moves fast, and will be eluted first. Small molecules, which are sucked into the pores, move slower and will be eluted later.

Sephadex G-50 (2.0 g, swelling for 3 hours at 20ºC before filling) or G200 (1.0 g, swelling for 5 hours at 90ºC before filling) was used as stationary phase followed by adding 3 mL illuminated reaction mixture which was promoted by CTAT/SDBS 20/80 vesicle with the total surfactant concentration at 5 mM. Yellow color fraction and the fractions right before and after the elution of yellow color solution were collected and analyzed by UV-Vis spectroscopy.

3.2.4 Interchangeable Reaction

3.2.4.1 AgNPs in CTAT-rich to SDBS-rich Vesicle

6 mL illuminated reaction mixture promoted by CTAT/SDBS 80/20 vesicle with a total surfactant concentration at 5 mM were prepared first. Next, 154.7 mg SDBS surfactant was added to that solution with vigorous stirring overnight, so that the stabilizer formulation changed to CTAT/SDBS 20/80. The alternation was achieved when the color of solution changed from yellow to brown.

3.2.4.2 AgNPs in SDBS-rich to CTAT-rich Vesicle

6 mL illuminated reaction mixture promoted by CTAT/SDBS 20/80 vesicle with the total surfactant concentration at 5 mM were prepared first. Next, 131.6 mg CTAT surfactant was added

to that solution with stirring for 5 minutes, until the color of solution changed from yellow to brown.

3.2.5 Characterization of AgNPs

3.2.5.1 UV-Vis Spectroscopy Analysis

The optical property of AgNPs was determined by UV-Vis spectrophotometer (HP 8452A Diode-Array Spectrophotometer with range of 190 to 820 nm with 2 nm resolution). UV quality quartz cuvettes, 1 cm path length, were used. The spectra of the reaction mixture containing $AgNO_3$, stabilizer, and I-2959 are recorded before and after irradiation, between 220 nm to 800 nm. Since a high concentration of mixture solution was used for synthesis, each UV absorption was recorded one more time with 10- fold dilute solution. Otherwise, the absorbance exceeded 1.0 and was unreliable because it was beyond the linear range of absorbance.

3.2.5.2 Dynamic Light Scattering (DLS)

Dynamic light scattering is a technique that involves detecting the scattered light of laser-illuminated sample at a known scattering angle θ to determine the average particle size of particles in a limited size range.

A computer-controlled particle size analyzer (NICOMP 380 ZLS) was used to analyze the size distribution of the yellow solution that was collected from the SEC column. This type of instrument can be used to determine the size of vesicle, thus it verified the presence of vesicle in that fraction. However, the analysis of size distribution of AgNPs was beyond the range of the instrument.

CHAPTER 4

LIGHT-ACTIVATED SURFACTANT-MEDIATED SYNTHESIS OF SILVER NANOPARTICLES

4.1 Overview

This chapter describes experiments aimed at evaluating the role of surfactants in the light activated synthesis of silver nanoparticles (AgNPs). The formation of silver nanoparticles is easily monitored by the onset of a strong, visible absorption band that is due to the surface plasmon resonance (SPR) that is characteristic of nanoscale silver particles and films. In this chapter, all spectra were acquired from a 10-fold diluted solution of the original reaction mixture to assure linearity unless otherwise indicated in legend.

Scaiano and co-workers pioneered the use of the photo-initiator, I-2959, in the synthesis of AgNPs in which ketyl radicals from I-2959 are photochemically generated and used to reduce silver salts to produce AgNPs. Initially, they demonstrated this method in organic solvents such as toluene.[23] More recently, they demonstrated a similar procedure in aqueous solutions of the surfactants CTAC and SDS.[34] In our project, we followed the method of Scaiano's group[34] to synthesize AgNPs and bimetallic nanoparticles of silver and gold. In our research, we repeated their experiment with SDS micelles and compared the results between SDS, SDBS, and CTAT micelles along with SDBS-rich and CTAT-rich surfactant vesicles. The findings from these experiments are discussed below.

4.2 AgNPs promoted by SDS and SDBS micelles

Following the procedure outlined by Gonzalez et al. (2009), we reproduced the synthesis of AgNPs in SDS micelles and next examined the role that the surfactant charge and aggregation

state (micelles versus vesicles) plays on the nanoparticle synthesis.

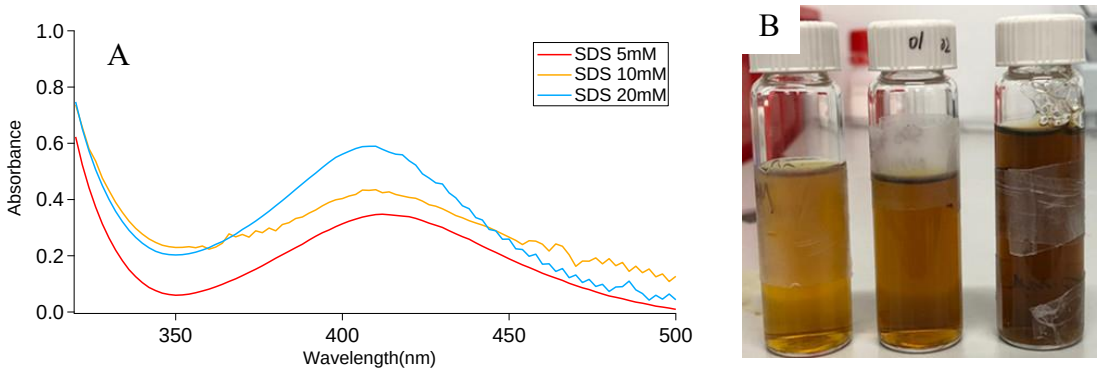

Figure 13. UV-vis analysis of reaction products from photo-initiated AgNP synthesis in SDS. A) UV-vis spectra of AgNP reaction mixtures in SDS at three surfactant concentrations. B) Photographs of the reaction mixtures after illumination with concentrations from left to right of 5.0 mM, 10.0 mM, and 20.0 mM.

Figure 13 shows the UV-vis spectrum acquired from the reaction mixture containing SDS, $AgNO_3$ and I-2959 after illumination. It can be clearly seen that there is a peak around 410 nm, which indicates the formation of AgNPs with a diameter of approximately 10 nm. Also shown are the images of three vials showing the color attributed to AgNPs and the effects of surfactant concentration in which the intensity of absorbance increases with higher SDS concentration. Panel 13B shows photographs of the resulting reaction mixtures after illumination demonstrating the solution color that arises from the SPR band. Note that the product yield, as shown by the SPR band intensity, increases with increasing surfactant concertation, and this is discussed in greater detail above. All preparations resulted in a stable, homogeneous solution, with no precipitates, right after illumination, whereas the product in high concentration of SDS starts to aggregate in 2 weeks as evidenced by the brown solution shown in Panel 13B.

Next, we compared the production of AgNPs in SDS with the same reaction but now using SDBS micelles rather than SDS. SDBS micelles were chosen because SDBS spontaneously undergoes a micelle-to-vesicle transition when the cationic surfactant, CTAT, is added in the

correct proportions. Our results show that SDBS micelles, also produce AgNPs as demonstrated in Figure 14.

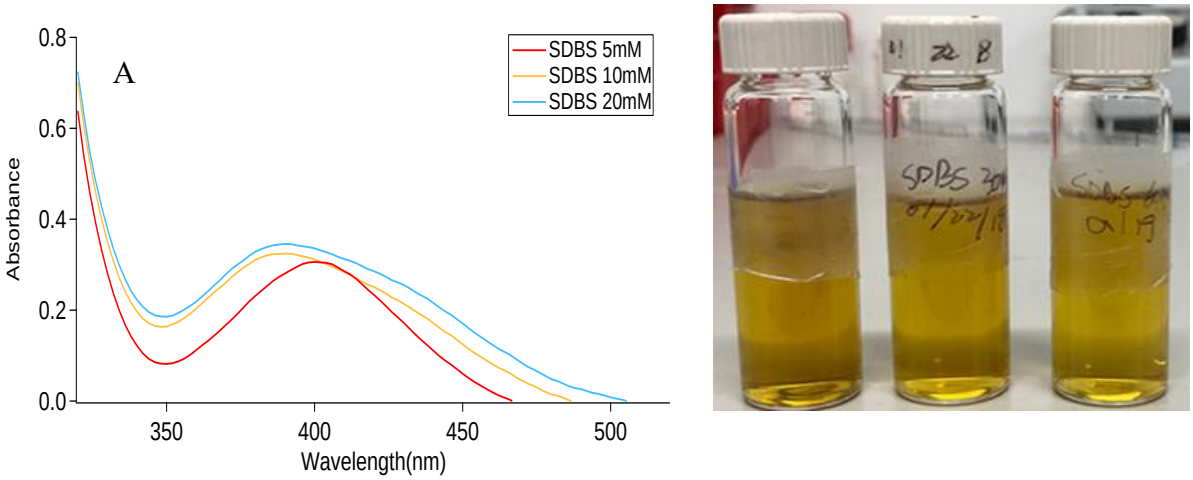

Figure 14. UV-vis analysis of reaction products from photo-initiated AgNP synthesis in SDBS. A) UV-vis spectra of AgNP reaction mixtures in SDBS at three surfactant concentrations. B) Photographs of the reaction mixtures after illumination with concentrations from left to right of 5.0 mM, 10.0 mM, and 20.0 mM.

SDBS has a CMC of 2.8mM, which is lower than that of SDS. Figure 14 shows the SPR band at 400 nm, indicating the presence of AgNPs. The peak has a blueshift when surfactant concentration is increased from 5 mM to 10 mM (from 400 nm to 390 nm), that suggests a decrease of nanoparticle size. However, the concentration of the SDBS micelle doesn't have a significant effect on the intensity of absorbance. All the products have the absorbance less than 0.4. Panel 14B is the digital photo of the product. Yellow color also confirms the formation of the silver nanoparticle. These particles are stable for months and can be reproducibly synthesized at room temperature.

4.3 Effect of Anionic Surfactant Concentration on AgNP Synthesis.

Next, we investigated the effects of surfactant concentration for both SDS and SDBS on the yield of AgNPs. In these experiments we systematically varied the surfactant concentration while holding all other factors constant. Figure 15 shows the results for SDS over the concentration

range of 2.0 to 160 mM. Panel 15A, shows the amplitude of the plasmon resonance as a function of SDS concentration. This graph shows a rapid increase in the plasmon band below the CMC of SDS (8.2 mM). Panel 15B, shows the absorbance spectrum and indicates that below the CMC at 2.0 and 3.0 mM, the spectrum is very broad and does not show a distinct plasmon band. This indicates that the presence of micelles, not merely surfactant monomers, is necessary for

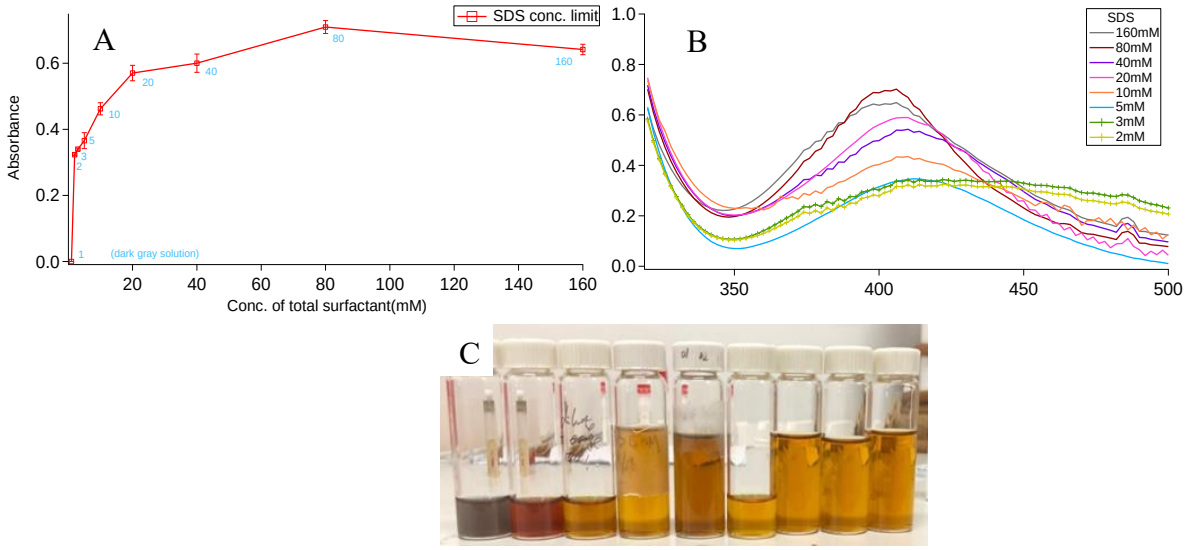

Figure15. Analysis of dependence for SDS surfactant. A) The amplitude of the plasmon resonance as a function of SDS concentration. B) UV-vis spectra of AgNP reaction mixtures in SDS at various surfactant concentrations from 2 mM to 160mM. C) Photographs of the reaction mixtures after illumination with concentrations from left to right of 1mM, 2 mM, 3 mM, 5 mM, 10 mM, 20 mM, 40 mM, 80 mM, and160 mM.

nanoparticle synthesis and indicates that aggregated surfactant promotes the reaction, presumably by solubilizing the initiator and keeping the reactants in close proximity as discussed further below.

Panel 15C shows the effects of concentration on the solution color and stability. At the lowest SDS concentration of 1.0 mM, the solution appears grey and has a broad and featureless spectrum. This spectrum is nearly identical to the spectrum acquired when the reaction is carried out in a surfactant-free aqueous preparation. Below 2.0 mM SDS, the spectrum is broad without a distinct SPR band and this is indicative of a broad particle size range. These observations can be explained by un-mediated growth of silver crystals due to the absence of surfactant that acts as a

passivating layer and inhibits continued crystal growth above the nanoscale. This is further supported by the observation that below 2.0 mM SDS, silver precipitation is observed during the reaction which occurs because larger-scale silver particles are forming.

In summary, the concentration dependent behavior with respect to SDS reveals two important observations: 1) below the CMC the production of AgNPs is not observed although reduction does occur, 2) near and above the CMC, AgNP production increases rapidly and then saturates at about 80 mM. These observations suggest that the micelle provides a unique environment for AgNP production. There are several roles that the micelle is likely playing. First

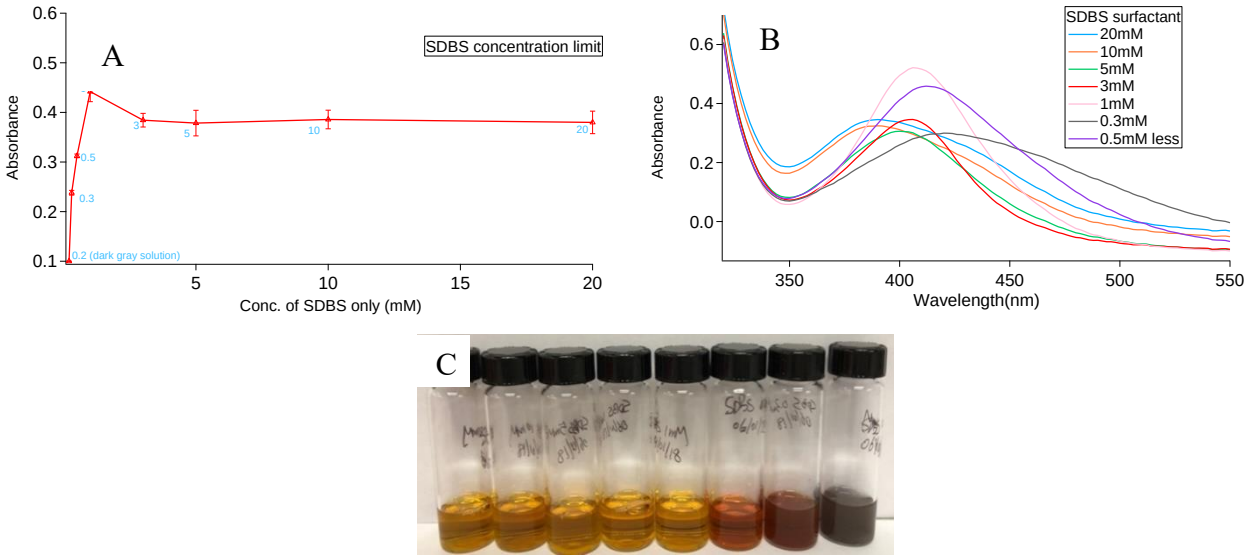

Figure 16. Analysis of dependence for SDBS surfactant. A) The amplitude of the plasmon resonance as a function of SDBS concentration. B) UV-vis spectra of AgNP reaction mixtures in SDBS at various surfactant concentrations from 2 mM to 160mM. C) Photographs of the reaction mixtures after illumination with concentrations from left to right of 20 mM, 10 mM, 5 mM, 3 mM, 1 mM, 0.5 mM, 0.3 mM, and 0.2 mM.

it provides an anionic interface that recruits silver cations in a counter-ion cloud around the micelle. Second, it solubilizes the I-2959. Third, it provides a passivating layer that limits nanoparticle growth to approximately 10 nm in diameter. The CMC of SDBS at 2.8 mM[42] is considerably lower than SDS at 8.2 mM.[34] If SDBS plays a similar role as SDS, as would be expected, then a similar concentration trend should be observed for both SDS and SDBS, simply altered by the value of

the CMC. The results for the concentration dependence of SDBS are shown in Figure 16.

Panel 16A, shows that for SDBS a similar trend to that of SDS is observed, but for SDBS the yield (as represented by the SPR absorbance) peaks at a much lower value of about 1.0 mM. This result is intriguing since it suggests that a much smaller addition of SDBS is necessary for good AgNP production. Panel 16B confirms that AgNPs are formed at the CMC of SDBS since a well-defined SPR band is seen at 2 mM. Figure 16C also shows that at concentrations below about 0.5 mM SDBS, well-defined AgNPs are not formed and the product resembles that achieved in aqueous solutions without surfactants or in solutions of SDS below 2.0 mM.

From a comparison of SDS and SDBS, it is clear that both anionic surfactants work well for AgNP synthesis. Overall, the AgNP yield appears to be about 50% higher in SDS, judging by the SPR signal amplitude at surfactant concentrations above their respective CMC values. However, AgNP production in SDS ceases below 2.0 mM but persists for SDBS down to 0.3 mM. This observation opens up an interesting line of inquiry regarding what are the best surfactants to use for AgNP production to achieve the purest sample, i.e. a sample with minimal surfactant and maximum AgNP concentration. This line of inquiry is pursued below.

Based on our observations, the anionic micelle is a useful platform for AgNP production. Presumably the reaction is facilitated by the clustering of silver cations around the anionic headgroups of a micelle. To test this theory, we conducted experiments using a cationic surfactant, CTAT and these results are discussed in the next section.

4.4 Effect of CTAT Micelle in AgNP Synthesis

The procedure used to produce AgNPs in anionic micelles was duplicated for the cationic surfactant CTAT (CMC = 0.34 mM).[42] Figure 17A shows the UV spectra of a reaction mixture

containing CTAT after illumination and reveals a broad peak with some evidence of an SPR band near 400 nm. However, the width of the absorbance and the color of the solution are again similar to the reaction product achieved in non-surfactant aqueous solutions. While it is clear that silver reduction occurs, the broad spectrum arises from a wide range of sizes and aggregation states. From the photo, it is clear to see that the solution, right after irradiation, is orange brownish, and after 2 hours it becomes brown with notable precipitate. Overnight, the particles completely precipitate. This precipitation implies the aggregation of silver. Thus, CTAT surfactant itself doesn't work for promoting a stable silver nanoparticle. In summary, CTAT does not promote AgNP formation as evidenced by the lack of a well-defined SPR band. Additionally, the product produced in CTAT solutions is similar to that produced in non-surfactant aqueous solutions and in very low concentration anionic surfactant solutions. Clearly the cationic surfactant is not suitable platform for AgNP production since it does not recruit silver cations and does not limit particle growth with surface passivation.

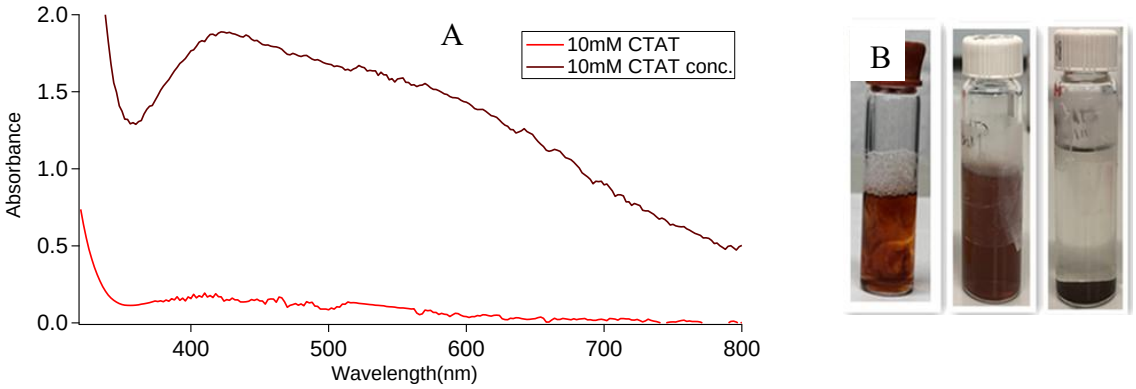

Figure 17. UV-vis analysis of reaction products from photo-initiated AgNP synthesis in CTAT at 10 mM. A) UV-vis spectra of AgNP reaction mixtures in CTAT at 10 mM. B) Photographs of the reaction mixtures after illumination from left to right for right after illumination, after 2 hours, overnight.

4.5 Mixed Surfactant Systems – "Catanionic" Vesicles.

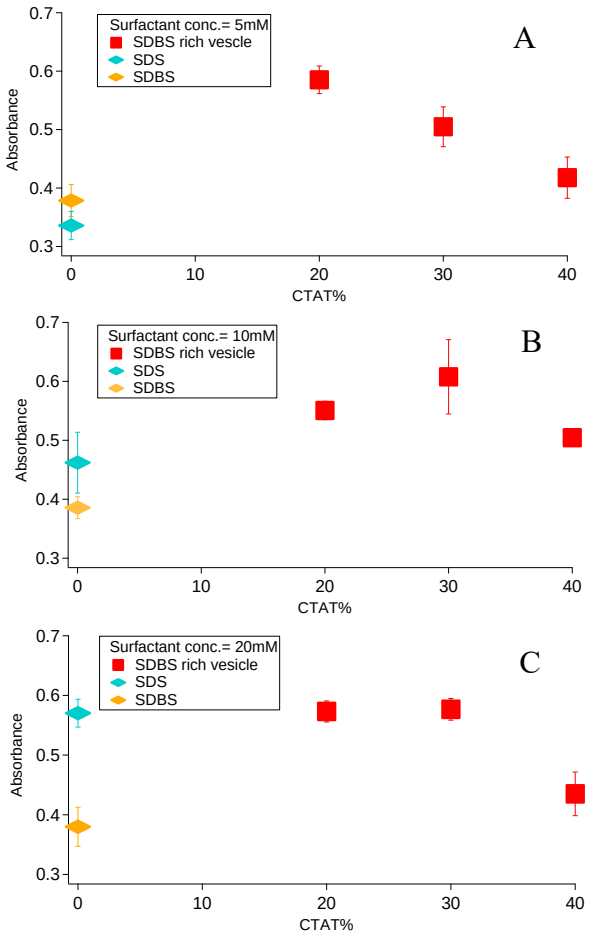

Figure 18. Comparison of SPR band value between negative charge micelles and vesicles. Error bars show the standard deviation of each formulation. A) The amplitude of the SPR as a function of CTAT% by mass in CTAT/SDBS mixture at 5mM. B) The amplitude of the SPR as a function of CTAT% by mass in CTAT/SDBS mixture at 10mM. C) The amplitude of the SPR as a function of CTAT% by mass in CTAT/SDBS mixture at

Next, we investigated the possibility of using a mixed surfactant system for AgNP synthesis. This attempt was motivated by the understanding that mixed surfactant systems of CTAT and SDBS form solutions that contain vesicles rather than micelles. The spontaneous formation of unilamellar vesicles from mixtures of CTAT and SDBS has been well investigated.[41-42] CTAT/SDBS mixtures form surfactant ion pairs that, when aggregated, pack into bilayers rather than micelles, much like dual-tailed surfactants such as phosphorlipids. At the correct proportions, these surfactant mixtures will aggregate to form unilamellar vesicles, which are spherical bilayer structures. This occurs when there is a molar excess of either the cation or anion, and therefore the vesicle bilayer will always have a net charge when formed from CTAT and SDBS.

Some potential advantages that a vesicle may have over a micelle in terms of promoting AgNP formation is that they have lower curvature and are much less dynamic with respect to exchange of monomers. In addition, the critical aggregation concentration is in the micromolar range, as compared to millimolar CMC's for CTAT or SDBS alone.

4.5.1 Effect of Anionic Surfactant Concentration on AgNP Synthesis

Figure 18 shows the SPR absorbance value after illumination as a function of CTAT composition in an SDBS/CTAT mixture. In these experiments the SDBS is always the major surfactant component and therefore the vesicles that form have a bilayer with a net negative charge. The panels in Figure 18, also show the yield for SDBS and SDS alone. In each panel the total surfactant concentration is fixed and noted in the legend.

Panel A shows an interesting trend. First, as discussed previously, the yield for SDBS is greater than SDS at this low concentration (5.0 mM) because this is below the CMC of SDS, but above that of SDBS. However, at this concentration, the inclusion of 20% CTAT results in an increase of AgNP production of ~150%. This remarkable increase in AgNP yield must be due to the transformation from micelles to vesicles. This increase occurs even though the concentration of SDBS is decreased, since the total surfactant concentration is constant. However, at 30% and 40% CTAT, the AgNP production decreases and this is likely due to the diminishing amount of SDBS relative to that of the 20% CTAT mixture. This finding indicates that the lower curvature and greater stability of the bilayer promotes AgNP synthesis far better than the high curvature, more dynamic and less stable micelle interface.

When the surfactant concentration is raised to 10 mM, the yield for pure SDS is now greater than that of pure SDBS, but still less than that of the 20% and 30% SDBS/CTAT vesicle solutions. Only when the SDS concentration is at 20 mM, does the yield approach that obtained with the mixed surfactant systems. But at 20 mM, the addition of CTAT to SDBS still dramatically increases the amplitude compared to the SDBS alone.

Figure 19A shows the dependence of the product yield as measured by the SPR absorption

on the total concentration of surfactant in a solution of with 20% CTAT. The trend is similar to that observed in Figures 15 and 16, but in this solution, the AgNPs are produced at much lower total surfactant concentrations. The spectra in Figure 19B show a well-defined plasmon band at total surfactant concentrations as low as 0.5 mM.

These findings show that this mixed surfactant system has some advantages over anionic

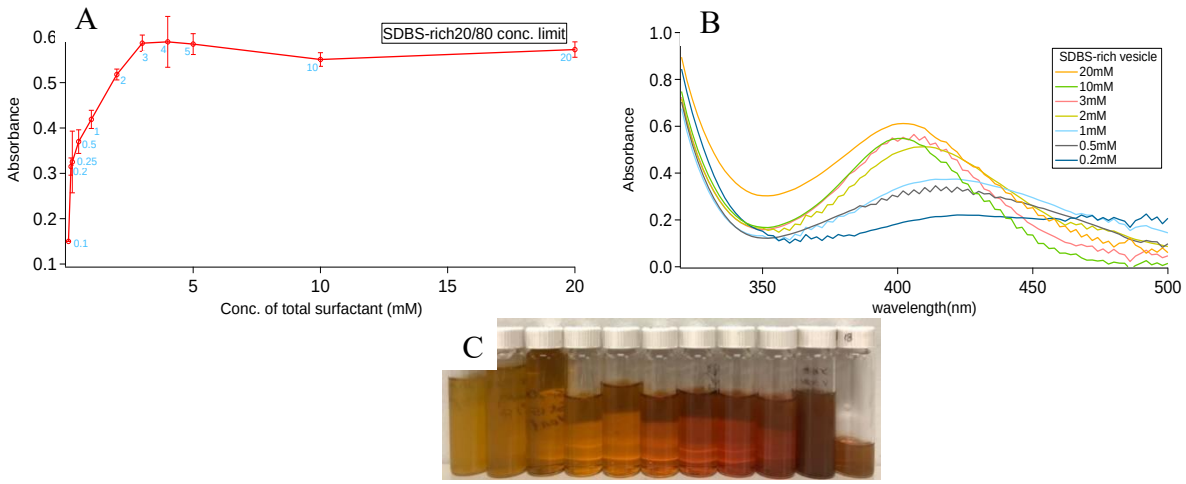

Figure 19. Analysis of dependence for SDBS-rich vesicle of with 20% CTAT at total surfactant concentration of 5mM. A) The amplitude of the plasmon resonance as a function of total surfactant concentration. B) UV-vis spectra of AgNP reaction mixtures in SDBS rich vesicle at various surfactant concentrations from 2 mM to 160mM. C) Photographs of the reaction mixtures after illumination with concentrations from left to right of 20 mM, 10 mM, 5 mM, 4 mM, 2 mM, 3 mM, 1 mM, 0.5 mM, 0.25 mM, 0.2 mM, and 0.1 mM.

micelles. Most notably, the mixed systems yield more AgNP at lower surfactant concentrations. In fact, the 20% CTAT solution at 5 mM total surfactant performs as well as 60 mM pure SDS (see Figure 15). Also, the use of less surfactant could be advantageous from a cost perspective and if the goal is to produce samples with minimal surfactant in the product.

All of the SDBS-rich vesicle preparations yielded products that show a good SPR band as shown in Figure 20, although there is a notable red shift and broadening of the SPR band as the CTAT concentration exceeds 20%. Also, all solutions yielded AgNPs that are colloidally stable, showing no precipitation for up to several weeks. Therefore, given the different preparations

investigated thus far; SDS micelles, SDBS micelles, CTAT micelles and SDBS-CTAT vesicles, the 20/80 CTAT-to-SDBS weight ratio appears to be the best formulation for yielding AgNPs at high yield with minimal added surfactant.

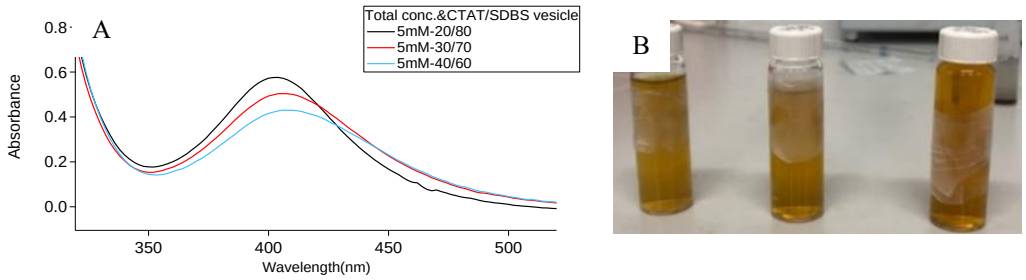

Figure 20. UV-vis analysis of reaction products from photo-initiated AgNP synthesis in CTAT/SDBS mixture of different ratio with total surfactant at 5 mM. A) UV-vis spectra of AgNP reaction mixtures containing three CTAT to SDBS ratios by mass with total concentration of surfactant at 5 mM. B) Photographs of the reaction mixtures after illumination of total surfactant concentrations at 5mM with different CTAT/SDBS mass ratio from left to right of CTAT/SDBS 20/80, 30/70, 40/60.

The reason for the higher yield observed in the vesicle-forming preparations is unclear and will require further study to elucidate. Tentatively, we suggest that the vesicles simply recruit more silver cations at the bilayer interface. This is because vesicles are less dynamic than micelles. The rate of change of a surfactant molecule between the aggregate and solution is approximately 3000 times slower in a bilayer than in a micelle. For instance, it has been shown that the life time of a surfactant molecule in vesicles is about 12 μs,[43] and in micelles is about 4 ns.[44] In addition, a vesicle contains a larger number of negative charges than a micelle and this facilitates the reaction since the proximity of the bilayer-solubilized photo initiator with reactive silver cations is improved.

4.5.2 AgNPs Promoted by Positively Charged Vesicle

Figure 21A shows the UV spectra of AgNPs that was generated in CTAT/SDBS mixture in where the CTAT is in excess with 80% of total surfactant concentration at 10mM, and thus it

forms positively charged vesicles. There is a broad peak with some evidence of an SPR band around 400 nm which indicates the occurrence of silver reduction, and the broad spectrum arises from a wide range of sizes and aggregation states.

This spectrum is very similar to the spectra of AgNPs promoted in CTAT micelles which

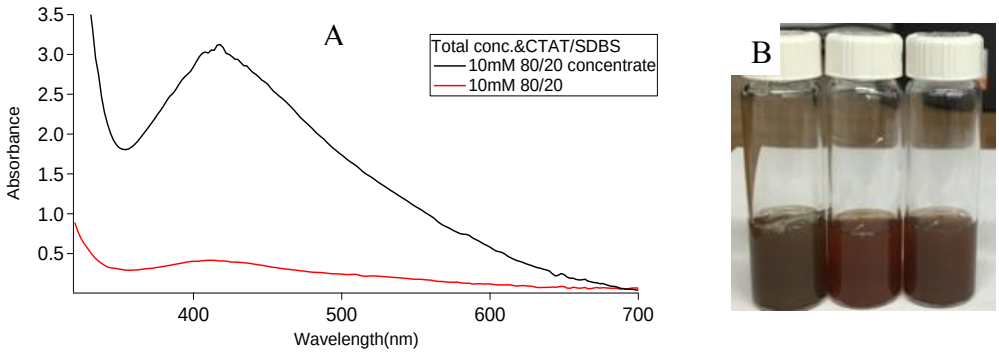

Figure 21. UV-vis analysis of reaction products from photo-initiated AgNP synthesis in CTAT-rich vesicle. A) UV-vis spectra of AgNP synthesis in CTAT/SDBS mixture with 80% CTAT by mass of total surfactant at 10 mM. B) Photographs of the reaction mixtures of total surfactant concentration at 10 mM with 3 CTAT/SDBS mass ratios from left to right for CTAT/SDBS 20/80, 30/70, 40/60

is shown in Figure 17 whereas this one has a higher absorbance which indicates that CTAT-rich vesicles yield more AgNPs than CTAT micelles. The 70/30 and 60/40 CTAT to SDBS mass ratio vesicles are also employed to produce AgNPs, and the spectra resulting from their illuminated reaction mixtures are similar to the 80/20 CTAT to SDBS mass ratio vesicles shown in Figure 21A. Figure 21B is the photo of the product. From the photo, it's clear to see that the solution is brown, the same as the color of AgNPs generated in CTAT micelles right after illumination. Surprisingly, AgNP in the CTAT-rich vesicle is stable for weeks with no precipitate, which is different from that in the CTAT micelle, which precipitates in 2 days. This observation suggests that the presence of SDBS surfactant, which has lower curvature and a less dynamic bilayer structure of the vesicle play a significant role to stabilize AgNPs. Thus, the CTAT-rich vesicle works for promoting stable AgNPs with a wide range of sizes. In short, CTAT-rich vesicle is better than the CTAT micelle but not as good as the SDBS-rich vesicle for AgNP production.

4.5.3 Interchangeable product

In these experiments, we varied the CTAT to SDBS ratio after illumination by adding appropriate amount of CTAT or SDBS surfactant to change the net charge of vesicle in the original reaction mixture. We find that AgNPs generated in the negative charge (SDBS-rich) vesicle and positive charge (CTAT-rich) vesicle are interchangeable.

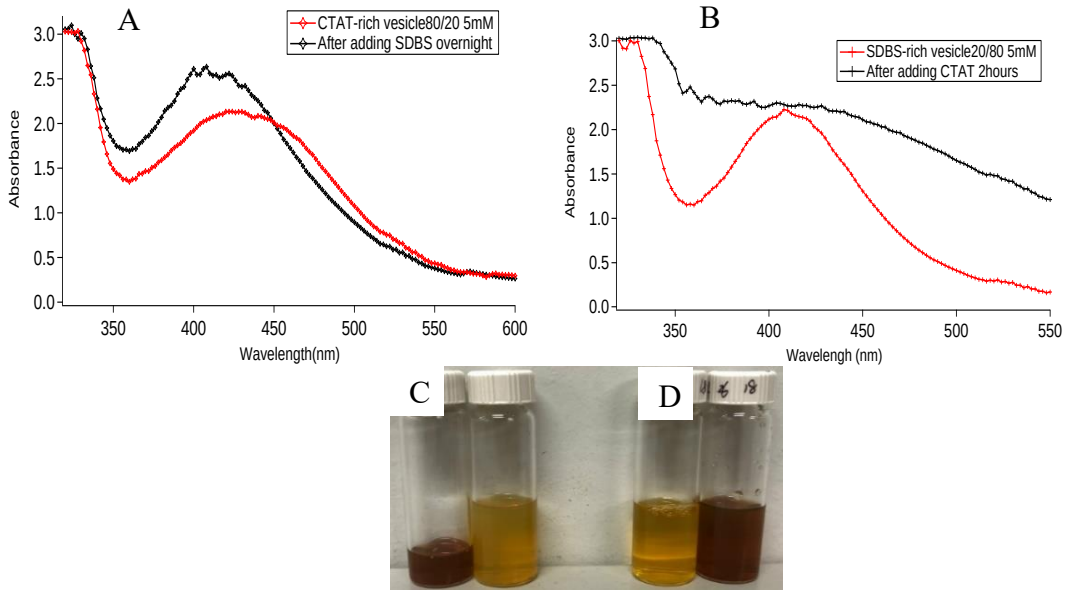

Figure 22. UV-vis analysis of products from photo-initiated AgNP synthesis in reversible reaction between positive charge and negative charge vesicles. A) UV-vis spectra of AgNP reaction mixtures from CTAT-rich to SDBS rich vesicles with total surfactant concentration at 5mM. B) UV-vis spectra of AgNP reaction mixtures from SDBS rich to CTAT-rich vesicles with total surfactant concentration at 5mM. C) Photographs of the reaction mixtures after illumination from left to right in CTAT-rich and converted SDBS-rich vesicles. D) Photographs of the reaction mixtures after illumination from left to right in SDBS-rich and converted CTAT-rich vesicles.

Panel 22A shows the UV-vis spectrum acquired from the illuminated reaction mixture containing CTAT-rich vesicles (80/20 CTAT to SDBS mass ratio with total surfactant concentration at 5 mM), and the reaction mixture containing SDBS-rich vesicles (20/80 CTAT to SDBS ratio) which is achieved by adding SDBS surfactant into the illuminated reaction mixture containing CTAT-rich vesicles followed by vigorous stirring overnight. There are two SPR bands in the spectrum: the red band is from the AgNPs generated in CTAT-rich vesicle originally, which

is the same as the band shows in figure 21A, and the black band comes from the same mixture after adding SDBS surfactant, therefore altering the net charge of vesicle from positive to negative. The black band has a blueshift with higher absorbance which is identical to the SPR band of AgNPs generated in the negatively charged vesicle at and above 3 mM. This is shown in Panel 19B. Panel 22C shows the color of solution before and after the addition of SDBS surfactant. It's clear to see that after adding SDBS surfactant, the color of solution changes from brown to yellow, the yellow color is characteristic for AgNPs in SDBS-rich vesicles which agrees with the band shift shown in panel 22A.

We tried the same experiment starting from AgNPs produced in SDBS-rich vesicle followed by the addition of CTAT surfactant until we obtained a CTAT-rich mixture which has 80/20 CTAT to SDBS ratio by mass. Panel 22B shows the UV spectra of initial AgNPs in SDBS-rich vesicle, and AgNPs in CTAT-rich mixture that is accomplished by adding CTAT surfactant in the original reaction mixture. The red band in Panel 22B is from AgNPs in SDBS-rich vesicle, and the black band is from the same solution after adding CTAT surfactant. The broad peak of the black band is characteristic for AgNPs promoted by CTAT-rich vesicle which is shown in Figure 21A. During the process, the color of the solution changes from yellow to brown which is shown in the photo in Figure 22D, and it confirms the variation of AgNPs in solution as well.

The observations above imply that AgNPs which are promoted in the positively charged and negatively charged vesicles are interchangeable, and the transition between them are achieved by altering the ratio of CTAT and SDBS surfactants. This reversible reaction is remarkable since it occurs after AgNPs are generated, and it confirms that the particle size and color are closely related to the capping agent and surrounding environment. This interchangeable product might be generated by changing the aggregation state of AgNPs. Additionally, it provides a method to

modify the size of nanoparticles after the synthesis.

4.5.4 Size Exclusion Chromatography

In this experiment, we investigate where the AgNP are generated in the reaction mixture containing catanionic vesicles. I.e. it is generated in the hydrophilic core of vesicle, in the bilayer, or outside of vesicle. To study how the AgNP related to vesicles, two mixture solutions are purified by Size-Exclusion Chromatography separately.

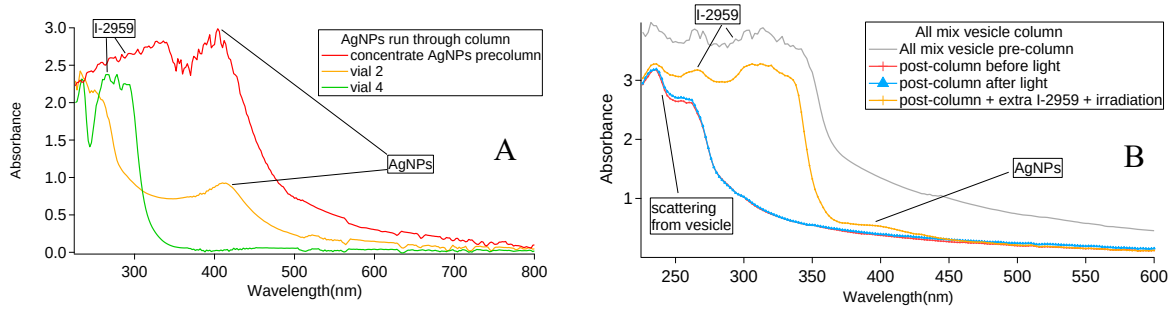

Figure 23. UV-vis analysis of fractions from SEC column. A) UV-vis analysis of reaction products purified from SEC column, from photo-initiated AgNP synthesis in SDBS-rich vesicles. B) UV-vis analysis of purified mixture solution by SEC column followed by irradiation.

First, the illuminated reaction mixture containing SDBS-rich vesicle (20/80 CTAT to SDBS ratio by mass) with total surfactant concentration at 5mM was prepared and passed through the column which uses Sephadex G-50 as stationary phase. Figure 23A shows the UV-vis spectra of different fractions from the column. It's clear to see that AgNPs come out in the 2nd vial as evidenced by the characteristic SPR band of AgNPs. With the help of the DLS technique, we confirmed that vesicles start to come out in the 2nd vial along with AgNPs. These observations might suggest two reasonable explanations. First, AgNPs are generated in vesicles since the vesicle has relatively larger size, thus coming out first. Second, the AgNP has similar size as vesicle therefore, they are coming out together. To find the correct explanation, the same reaction mixture before the illumination is purified by the same column. The sample is collected as the vesicle starts

to come out and followed by illumination. The UV spectra of various fractions is shown in Panel 23B. If there are AgNPs generated after irradiation, the first explanation is proved. Regrettably, there is no AgNP formed after illumination as evidenced by the lack of a well-defined SPR band and a yellow solution. Therefore, this observation disagrees with the first explanation above. However, these two spectra reveal that I-2959 doesn't come out with vesicles in the 2nd vial as evidenced by the lack of a characteristic peak of I-2959 around 270 nm, which suggests that even though I- 2959 is a water soluble photoinitiator, it doesn't like to stay in the vesicle. No AgNP generated from the illuminated sample of the second column is due to the lack of photoinitiator in the mixture solution (the blue and red band are shown in Panel 23B).

In short, this experiment suggests that AgNPs associate with vesicles since without vesicles AgNPs are unstable in solution resulting in an aggregation. In addition, I-2959, a water soluble photoinitiator, is favorable to be retained and stabilized in the bilayer of vesicle.

CHAPTER 5

CONCLUSION

In this thesis, we used various surfactant-based stabilizers to promote photo-induced synthesis of silver nanoparticles and investigated the role that surfactant charge plays in the synthesis. The reaction is activated by the irradiation of the reaction mixture containing photoinitiator, I-2959, to obtain ketyl radicals which reduce silver salts to produce AgNPs. The formation of silver nanoparticles is confirmed by the color change of the reaction mixture as well as the appearance of a strong, visible absorption band around 400 nm that is because of the surface plasmon resonance (SPR) that is characteristic of AgNPs. The employed stabilizing agent include SDS, SDBS, and CTAT surfactants along with SDBS-rich and CTAT-rich surfactant vesicles. Various stabilizers give rise to different results. The negative charge micelles, SDS and SDBS, are favorable for promoting AgNPs above the CMC because its anionic interface recruits silver cations in a counter-ion cloud and inhibits the overgrowth of AgNPs. Cationic surfactant, CTAT, is not suitable for the synthesis, and CTAT-rich vesicle promotes AgNPs in a large range of sizes. The SDBS-rich vesicle promotes high yield AgNPs with minimal added surfactant. Therefore, it is concluded to be the best formulation studied for yielding AgNPs. This result is remarkable since the use of less surfactant leads to a low-cost synthesis and it also decreases the limiting concentration of stabilizer involved in the reaction. In addition, we find that the AgNP which is generated in CTAT-rich and SDBS-rich vesicle are interchangeable. This is probably because of the variation of the aggregation state of AgNPs.

Future work will involve TEM studies regarding the size determination of synthesized AgNPs.

REFERENCES

REFERENCES

1. Freestone, I.; Meeks, N.; Sax, M.; Higgitt, C., The Lycurgus cup—a roman nanotechnology. *Gold bulletin* **2007,** *40* (4), 270-277.

2. Lombardo, D.; Kiselev, M. A.; Magazù, S.; Calandra, P., Amphiphiles self-assembly: basic concepts and future perspectives of supramolecular approaches. *Advances in Condensed Matter Physics* **2015,** *2015*.

3. Murphy, C. J., Nanocubes and nanoboxes. *Science* **2002,** *298* (5601), 2139-2141.

4. Faraday, M., X. The Bakerian Lecture.—Experimental relations of gold (and other metals) to light. *Philosophical Transactions of the Royal Society of London* **1857,** *147*, 145-181.

5. Xia, Y.; Xiong, Y.; Lim, B.; Skrabalak, S. E., Shape-controlled synthesis of metal nanocrystals: Simple chemistry meets complex physics? *Angewandte Chemie International Edition* **2009,** *48* (1), 60-103.

6. Noguez, C., Surface plasmons on metal nanoparticles: the influence of shape and physical environment. *The Journal of Physical Chemistry C* **2007,** *111* (10), 3806-3819.

7. Kelly, K. L.; Coronado, E.; Zhao, L. L.; Schatz, G. C., The optical properties of metal nanoparticles: the influence of size, shape, and dielectric environment **2003**.

8. Burda, C.; Chen, X.; Narayanan, R.; El-Sayed, M. A., Chemistry and properties of nanocrystals of different shapes. *Chemical reviews* **2005,** *105* (4), 1025-1102.

9. Alexander, J. W., History of the medical use of silver. *Surgical infections* **2009,** *10* (3), 289-292.

10. Rai, M.; Yadav, A.; Gade, A., Silver nanoparticles as a new generation of antimicrobials. *Biotechnology advances* **2009,** *27* (1), 76-83.

11. Dastjerdi, R.; Montazer, M., A review on the application of inorganic nano-structured materials in the modification of textiles: focus on anti-microbial properties. *Colloids and Surfaces B: Biointerfaces* **2010,** *79* (1), 5-18.

12. Duncan, T. V., Applications of nanotechnology in food packaging and food safety: barrier materials, antimicrobials and sensors. *Journal of colloid and interface science* **2011,** *363* (1), 1-24.

13. Madaria, A. R.; Kumar, A.; Zhou, C., Large scale, highly conductive and patterned transparent films of silver nanowires on arbitrary substrates and their application in touch screens. *Nanotechnology* **2011,** *22* (24), 245201.

14. Austin, L. A.; Mackey, M. A.; Dreaden, E. C.; El-Sayed, M. A., The optical, photothermal, and facile surface chemical properties of gold and silver nanoparticles in biodiagnostics, therapy, and drug delivery. *Archives of toxicology* **2014,** *88* (7), 1391-1417.

15. Suh, Y. D.; Jung, J.; Lee, H.; Yeo, J.; Hong, S.; Lee, P.; Lee, D.; Ko, S. H., Nanowire reinforced nanoparticle nanocomposite for highly flexible transparent electrodes: borrowing ideas from macrocomposites in steel-wire reinforced concrete. *Journal of Materials Chemistry C* **2017,** *5* (4), 791-798.

16. Yang, Y.; Westerhoff, P., Presence in, and release of, nanomaterials from consumer products. In *Nanomaterial*, Springer: **2014**; pp 1-17.

17. Prabhu, S.; Poulose, E. K., Silver nanoparticles: mechanism of antimicrobial action, synthesis, medical applications, and toxicity effects. *International nano letters* **2012,** *2* (1), 32.

18. de Alwis Weerasekera, H.; Griffith, M.; Alarcon, E. I., Biomedical uses of silver nanoparticles: from roman wine cups to biomedical devices. In *Silver Nanoparticle Applications*, Springer: **2015**; pp 93-125.

19. Sotiriou, G. A.; Pratsinis, S. E., Engineering nanosilver as an antibacterial, biosensor and bioimaging material. *Current opinion in chemical engineering* **2011,** *1* (1), 3-10.

20. Mathew, T. V.; Kuriakose, S., Studies on the antimicrobial properties of colloidal silver nanoparticles stabilized by bovine serum albumin. *Colloids and Surfaces B: Biointerfaces* **2013,** *101*, 14-18.

21. Moisan, M.; Barbeau, J.; Moreau, S.; Pelletier, J.; Tabrizian, M.; Yahia, L. H., Low-temperature sterilization using gas plasmas: a review of the experiments and an analysis of the inactivation mechanisms. *International journal of Pharmaceutics* **2001,** *226* (1-2), 1-21.

22. Alqadi, M.; Noqtah, O. A.; Alzoubi, F.; Alzouby, J.; Aljarrah, K., pH effect on the aggregation of silver nanoparticles synthesized by chemical reduction. *Materials Science-Poland* **2014,** *32* (1), 107-111.

23. Maretti, L.; Billone, P. S.; Liu, Y.; Scaiano, J. C., Facile photochemical synthesis and characterization of highly fluorescent silver nanoparticles. *Journal of the American Chemical Society* **2009,** *131* (39), 13972-13980.

24. Pacioni, N.; Borsarelli, C.; Rey, V.; Veglia, A., Synthetic Routes for the Preparation of Silver Nanoparticles: A Mechanistic Perspective. *Silver Nanoparticle applications: In the fabrication and design of medical and Biosensing devices; Udekwu, KI, Alarcón, E. l, Griffith, M., Eds* **2012**.

25. Zoski, C. G., *Handbook of electrochemistry*. Elsevier: **2006**.

26. Nazeruddin, G.; Prasad, N.; Waghmare, S.; Garadkar, K.; Mulla, I., Extracellular biosynthesis of silver nanoparticle using Azadirachta indica leaf extract and its anti-microbial activity. *Journal of Alloys and Compounds* **2014,** *583*, 272-277.

27. Zhang, W., Nanoparticle aggregation: principles and modeling. In *Nanomaterial*, Springer: **2014**; pp 19-43.

28. Turkevich, J.; Stevenson, P. C.; Hillier, J., A study of the nucleation and growth processes in the synthesis of colloidal gold. *Discussions of the Faraday Society* **1951,** *11*, 55-75.

29. Brust, M.; Walker, M.; Bethell, D.; Schiffrin, D. J.; Whyman, R., J. of the Chemical Society. *Chemistry Communications* **1994,** *801*.

30. Zhao, P.; Li, N.; Astruc, D., State of the art in gold nanoparticle synthesis. *Coordination Chemistry Reviews* **2013,** *257* (3-4), 638-665.

31. Frens, G., Controlled nucleation for the regulation of the particle size in monodisperse gold suspensions. *Nature physical science* **1973,** *241* (105), 20.

32. Brown, K. R.; Fox, A. P.; Natan, M. J., Morphology-dependent electrochemistry of cytochrome c at Au colloid-modified SnO2 electrodes. *Journal of the American Chemical Society* **1996,** *118* (5), 1154-1157.

33. Marin, M. L.; McGilvray, K. L.; Scaiano, J. C., Photochemical strategies for the synthesis of gold nanoparticles from Au (III) and Au (I) using photoinduced free radical generation. *Journal of the American Chemical Society* **2008,** *130* (49), 16572-16584.

34. Gonzalez, C. M.; Liu, Y.; Scaiano, J., Photochemical Strategies for the Facile Synthesis of Gold− Silver Alloy and Core− Shell Bimetallic Nanoparticles. *The Journal of Physical Chemistry C* **2009,** *113* (27), 11861-11867.

35. Alarcon, E. I.; Bueno-Alejo, C. J.; Noel, C. W.; Stamplecoskie, K. G.; Pacioni, N. L.; Poblete, H.; Scaiano, J., Human serum albumin as protecting agent of silver nanoparticles: role of the protein conformation and amine groups in the nanoparticle stabilization. *Journal of nanoparticle research* **2013,** *15* (1), 1374.

36. Clint, J. H., Nature of surfactants. In *Surfactant Aggregation*, Springer: **1992**; pp 1-12.

37. Israelachvili, J. N.; Mitchell, D. J.; Ninham, B. W., Theory of self-assembly of hydrocarbon amphiphiles into micelles and bilayers. *Journal of the Chemical Society, Faraday Transactions 2: Molecular and Chemical Physics* **1976,** *72*, 1525-1568.

38. Šegota, S., Spontaneous formation of vesicles. *Advances in colloid and interface science* **2006,** *121* (1-3), 51-75.

39. Bangham, A.; Hill, M.; Miller, N., Preparation and use of liposomes as models of biological membranes. In *Methods in membrane biology*, Springer: **1974**; pp 1-68.

40. Kaler, E. W.; Murthy, A. K.; Rodriguez, B. E.; Zasadzinski, J., Spontaneous vesicle formation in aqueous mixtures of single-tailed surfactants. *Science* **1989,** *245* (4924), 1371-1374.

41. Wang, Z.; Leung, M. H.; Kee, T. W.; English, D. S., The role of charge in the surfactant-assisted stabilization of the natural product curcumin. *Langmuir* **2009,** *26* (8), 5520-5526.

42. Lioi, S. B.; Wang, X.; Islam, M. R.; Danoff, E. J.; English, D. S., Catanionic surfactant vesicles for electrostatic molecular sequestration and separation. *Physical Chemistry Chemical Physics* **2009,** *11* (41), 9315-9325.

43. Söderman, O.; Herrington, K. L.; Kaler, E. W.; Miller, D. D., Transition from micelles to vesicles in aqueous mixtures of anionic and cationic surfactants. *Langmuir* **1997,** *13* (21), 5531-5538.

44. Novo, M.; Felekyan, S.; Seidel, C. A.; Al-Soufi, W., Dye-exchange dynamics in micellar solutions studied by fluorescence correlation spectroscopy. *The Journal of Physical Chemistry B* **2007,** *111* (14), 3614-3624.